Multiple band structures in ^{68}Ge

A. P. de Lima, A. V. Ramayya, J. H. Hamilton, B. Van Nooijen,† R. M. Ronningen,‡ H. Kawakami,§ R. B. Piercey, and E. de Lima‖
Physics Department, Vanderbilt University, Nashville, Tennessee 37235

R. L. Robinson and H. J. Kim
Physics Division, Oak Ridge National Laboratory, Oak Ridge, Tennessee 37830

L. K. Peker
NNDC, Brookhaven National Laboratory, Upton, New York 11973

F. A. Rickey and R. Popli
Physics Department, Purdue University, West Lafayette, Indiana 47907

A. J. Caffrey
Physics Department, The Johns Hopkins University, Baltimore, Maryland 21218

J. C. Wells
Physics Department, Tennessee Technological University, Cookeville, Tennessee 38501
and Physics Division, Oak Ridge National Laboratory, Oak Ridge, Tennessee 37830
(Received 14 July 1980)

Low- and high-spin states of ^{68}Ge are investigated through in-beam γ-ray spectroscopy via the ^{58}Ni(^{12}C,2p), ^{63}Cu(^{7}Li,2n), and ^{52}Cr(^{19}F,$p2n$) reactions. A surprising richness of collective bands is observed in ^{68}Ge including three even parity bands built on 8^+ levels, the lower two of which are assigned as rotational aligned bands built on both proton and neutron $(g_{9/2})^2$ configurations, and three odd parity bands built on π and ν configurations that include the $g_{9/2}$ orbit. Details of the multiple bands and other levels observed in ^{68}Ge are presented. Rotation-aligned model calculations and interacting boson model calculations for ^{68}Ge are also described.

[NUCLEAR REACTIONS ^{58}Ni(^{12}C,2p), E=39 MeV; ^{63}Cu(^{7}Li, 2n), E=18 MeV; ^{52}Cr(^{19}F, $p2n$), E=50 MeV. Measured E_γ, I_γ,$\gamma(\theta)$, $\gamma-\gamma(\theta)$,P, Doppler line shapes. ^{68}Ge levels, J, π, δ, $T_{1/2}$ deduced. IBA calculations, RAL calculations.]

I. INTRODUCTION

In a recent letter[1] and earlier conference reports,[2-4] we reported that the yrast cascade above the 6^+ level in ^{68}Ge triple forks into three 8^+ levels. The bands built on the two lowest 8^+ levels exhibit backbending in their moment of inertia plots at the 8^+ level while the third band does not. These two lower bands were interpreted as the first evidence for both proton and neutron rotation-aligned bands built on the same orbital in one nucleus.[1] In this paper we report the details of the evidence for these bands and other features of the levels observed in ^{68}Ge. The following reactions were studied in our investigations: ^{58}Ni(^{12}C, 2p)^{68}Ge, ^{63}Cu(^{7}Li, 2n)^{68}Ge, and ^{52}Cr(^{19}F,$p2n$)^{68}Ge. Indeed, a surprising richness of bands is observed in ^{68}Ge in these reactions. Previously, ^{68}Ge had been studied by the ^{58}Ni(^{12}C, 2p) (Refs. 5 and 6) and ^{40}Ca(^{32}S, 2p) (Ref. 5) reactions, the beta decay of ^{68}As which populates states up to 4^+, and the ^{70}Ge(p,t) reaction.[7,8] Simultaneously with our work, ^{68}Ge was studied by Morand *et al.*[9] through the ^{66}Zn(α, 2n) reaction, by Pardo *et al.*[10] through the decay of ^{68}As, and by Guilbault *et al.*[11] through the (p,t) reaction.

Prior to our work, little was known about high-spin states in ^{68}Ge. The spins in the yrast band had been definitely established[5,6] only to 4^+ with a tentative 6^+ (Refs. 5 and 6) and one tentatively assigned[6] 8^+ level above that. Our work yields three positive parity bands and extends them to a tentative 14^+ level and two negative parity bands to two tentative 11^- states. Quasiparticle plus rotor calculations were performed.[1] These calculations provide a reasonable explanation of the triple forking and the three negative parity bands. Details of the two-quasiparticle-plus-rotor calculations for ^{68}Ge also are given in this paper along with recent interacting boson model calculations.

II. EXPERIMENTAL PROCEDURES AND RESULTS

In-beam, gamma-ray spectroscopy experiments, including γ-ray yield and angular distribution, gamma-gamma coincidence, gamma-gamma angular correlation (DCO), and lifetime measure-

ments were made via the reaction ^{58}Ni(^{12}C, 2p)^{68}Ge with a beam energy of 39 MeV. Angular distribution studies via the ^{63}Cu(^{7}Li, 2n)^{68}Ge reaction at 18 MeV and gamma-gamma coincidence and lifetime studies via the ^{52}Cr(^{19}F, p2n)^{68}Ge reaction at 50 MeV also were made. These experiments were carried out at the Oak Ridge National Laboratory EN Tandem Van de Graaff accelerator facility. The targets used were 0.2–0.6 mg/cm^2 of enriched material evaporated onto thick Pt backings. The Ge(Li) detectors typically had a resolution of 2.5 keV at 1.33 MeV and an efficiency of 18 to 23% of a 7.6 × 7.6 cm NaI detector at 1.33 MeV.

The different choices of beam energies were based on a preliminary analysis of the relative yields of the 1428-keV ($6^+ \rightarrow 4^+$) transition. The yield of γ rays from the ^{58}Ni(^{12}C, 2p) reaction was obtained over the energy range 31.5 to 41.5 MeV.

The singles gamma-ray spectrum from the ^{58}Ni(^{12}C, 2p) reaction at 55° from the beam direction is presented in Fig. 1. The energies and intensities are given in Table I. The bold numbers in Fig. 1 refer to transitions placed in the ^{68}Ge level scheme which is shown in Fig. 2.

For the gamma-gamma coincidence studies, the two Ge(Li) detectors were placed at 0° and 90° to the beam direction at a target-to-detector distance of 5 cm. The coincidence events were stored in a CDC 3200 computer through the buffer memory of a PDP-11, as a 1024 by 1024 matrix. Our gamma-gamma coincidence run with the ^{52}Cr(^{19}F, 2pn) reaction was expected to improve the population of the high spin states since the angular momentum of the compound nucleus was much higher. This experiment was also expected to give Doppler tails large enough to be analyzed from the coincidence gates, to help avoid the problems associated with different feeding times of the side feeders and contaminant lines which may be present on the singles data. Although it was observed that ^{68}Ge was indeed the strongest channel in this reaction, the peak to background ratios were smaller than those observed in the ^{58}Ni (^{12}C, 2p) reaction. This fact may be explained by the increase in the number of exit channels present in this reaction because of the higher energy and angular momentum of the compound nucleus formed. The analysis of gated spectra from this coincidence experiment showed features similar to those obtained with the ^{58}Ni(^{12}C, 2p) reaction.

The gamma-ray angular distribution data were taken at 0°, 55°, and 90° relative to the incident beam direction. A second Ge(Li) detector, placed at 270°, was used as a monitor for normalization purposes. The angular distribution coefficients A_k were extracted by solving the function $W(\theta) = [1 + \sum_{k=2,4} \alpha_k g_k A_k P_k(\cos\theta)]$ for the three angles,

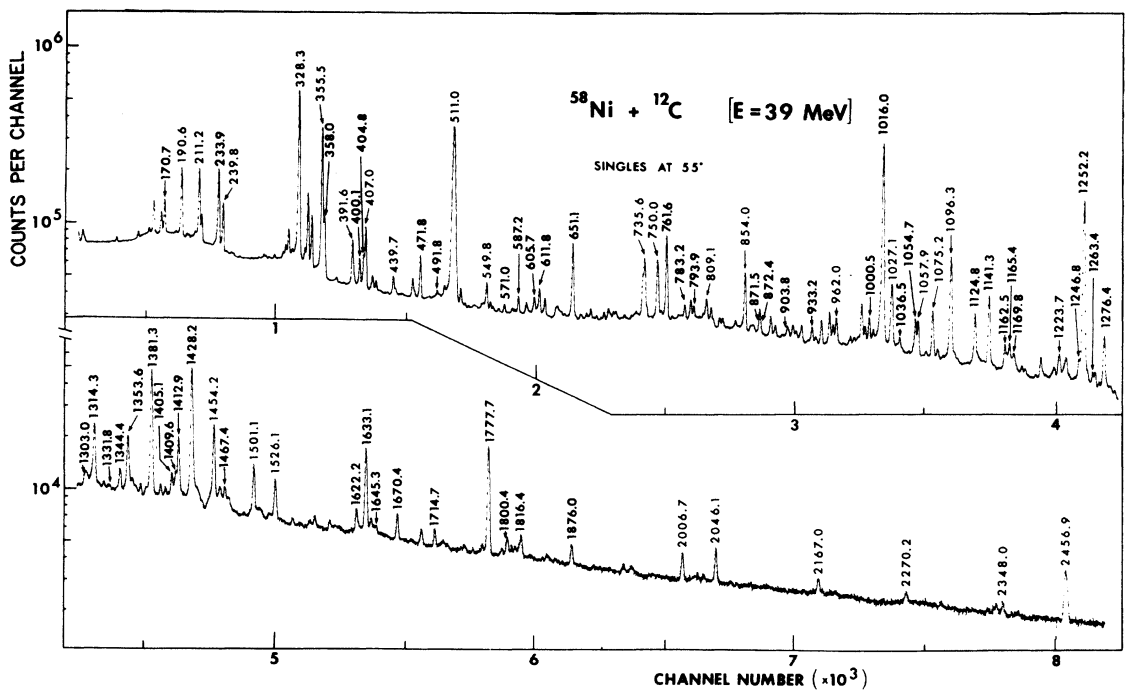

FIG. 1. Singles gamma-ray spectrum from the ^{58}Ni(^{12}C, 2p) reaction at a beam energy of 39 MeV. The bold numbers refer to transitions placed in the ^{68}Ge level scheme. The other energy values are only given for strong γ rays.

TABLE I. Angular distribution coefficients of γ rays in ^{68}Ge from the reaction ^{58}Ni(^{12}C, $2p$)^{68}Ge at 39 MeV. The spins, parities, multipolarities, mixing ratios, and attenuation coefficients are also given.

E_γ	Intensity	A_2	A_4	$J_i \rightarrow J_f$		E/M	δ	α_2
171	9.8(15)	−0.171(15)	0.007(2)	7^-	6^-	$M1,E2$	0.04(2)	0.76
234	17.6(18)							
358	2.0(5)							
400	2.82(18)	0.368(16)	0.004(18)	7^-	7^-	$M1,E2$	0.5(2)	0.62(3)
405	3.11(16)	0.34(2)	−0.12(4)	7^-	5^-	$E2$		0.77
472	5.08(25)	0.34(2)	−0.10(3)	7^-	5^-	$E2$		0.77
492	0.67(8)							
571	0.68(8)							
587	1.31(9)							
606	1.91(11)	0.275(23)	−0.038(26)	(9^-)	7^-	$E2$		0.68(6)
612	2.90(14)	0.117(23)	−0.073(26)	(4^+)	3^+	$M1,E2$	0.24(4)	0.57
632	0.35(10)							
651	11.07(50)	−0.105(12)	0.018(14)	3^+	2^+	$M1,E2$	0.06(2)	0.40
702	0.79(10)							
738	1.17(10)							
750	1.10(20)							
762	14.40(75)	0.072(10)	−0.002(13)	2^+	2^+	$M1,E2$	−0.15(3)	0.25
783	1.30(10)							
794	1.30(11)							
872	0.50(15)							
872	1.00(25)							
904	0.92(13)							
933	1.51(10)	0.32(6)	−0.05(6)	5^-	3^-	$E2$		0.64
1000	2.45(12)	0.35(4)	−0.08(4)	5^-	3^-	$E2$		0.71
1016	100(5)	0.210(12)	−0.056(14)	2^+	0^+	$E2$		0.29
1036	1.36(9)							
1055	4.04(20)							
1075	6.26(31)	0.312(25)	−0.07(3)	8^-	6^-	$E2$		0.73
1096	2.50(50)							
1125	6.71(33)	0.32(5)	−0.10(5)	10^+	8^+	$E2$		0.79
1141	9.85(50)	0.324(28)	−0.117(45)	8^+	6^+	$E2$		0.76
1163	1.85(15)							
1165	3.33(20)	0.32(10)	−0.17(12)	(10^+)	8^+	$E2$		0.77
1170	1.10(12)							
1224	3.48(20)	0.29(5)	−0.11(7)	(9^-)	7^-	$E2$		0.72
1247	2.43(15)							
1252	59.0(35)	0.317(18)	−0.071(21)	4^+	2^+	$E2$		0.62
1263	1.32(25)							
1276	7.14(36)	0.321(41)	−0.10(5)	(9^-)	7^-	$E2$		0.79
1303	0.83(14)							
1314	6.69(33)	−0.151(24)	−0.01(4)	5^-	4^+	$E1,M2$	0.04(3)	0.60
1332	0.26(5)							
1344	2.37(12)	0.244(50)	−0.064(55)	(12^+)	10^+	$E2$		0.60
1354	6.61(33)	0.357(30)	−0.120(41)	8^+	6^+	$E2$		0.83
1381	17.36(87)	−0.293(24)	−0.014(25)	5^-	4^+	$E1,M2$	0.04(2)	0.69
1405	1.24(9)	0.205(21)	−0.063(24)	4^+	2^+	$E2$		0.39(4)
1410	1.15(10)	0.256(61)	−0.088(70)	(12^+)	10^+	$E2$		0.63
1413	4.05(21)	−0.020(16)	−0.002(23)	3^+	2^+	$M1,E2$	0.16(8)	0.40
1428	22.70(11)	0.303(25)	−0.11(4)	6^+	4^+	$E2$		0.67
1467	1.28(10)	0.28(6)	−0.05(7)	(11^-)	(9^-)	$E2$		0.69
1622	1.28(10)							
1633	6.81(40)	−0.107(10)	−0.020(15)	3^-	2^+	$E1,M2$	0.09(3)	0.47
1645	0.34(5)							
1670	1.39(10)	0.31(5)	−0.11(5)	8^+	6^+	$E2$		0.76
1715	0.86(8)	0.34(5)	−0.13(6)	(11^-)	(9^-)	$E2$		0.84
1778	9.10(50)	0.150(10)	−0.014(12)	2^+	0^+	$E2$		0.21
1800	0.40(15)	0.31(6)	−0.08(7)	(14^+)	(12^+)	$E2$		0.78
1816	1.35(12)	0.141(31)	0.01(4)	4^+	2^+	$E2$		0.28
1876	0.84(9)	0.25(10)	−0.05(6)	(10^+)	8^+	$E2$		0.62

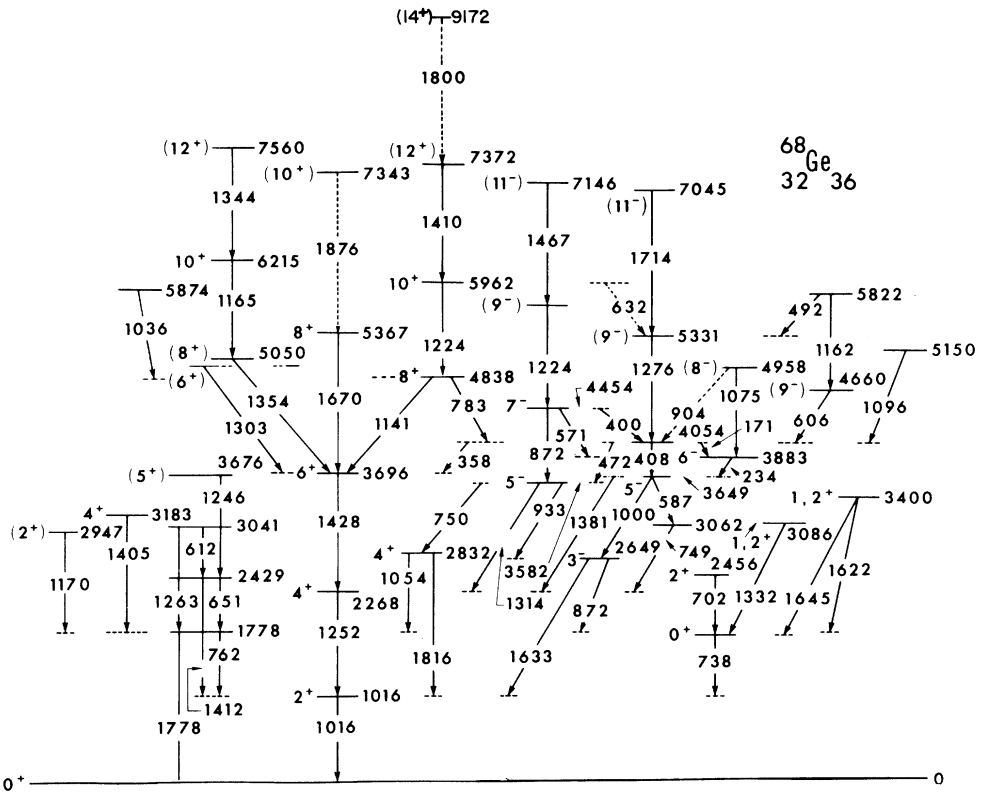

FIG. 2. The energy level diagram of ^{68}Ge obtained in the present experiment. The γ-ray intensities are obtained from the ^{12}C + ^{58}Ni experiment.

where α_k's are the alignment parameters and g_k's the solid angle corrections. The angular distribution and attenuation coefficients extracted from the ^{58}Ni + ^{12}C reaction are presented in Tables I and II. Table III shows the angular distribution results of the ^{68}Ge gamma rays obtained from the reaction ^{63}Cu(^{7}Li, $2n$)^{68}Ge at 18 MeV. The attenuation coefficients obtained from the angular distributions were used in the calculation of the theoretical DCO ratios.[12] Directional correlation from oriented nuclei (DCO) data were extraced from the gamma-gamma coincidence experiment. For the choice of angles used, the experimental DCO ratio is defined as

$$R = \frac{W(90, 0)}{W(0, 90)}, \qquad (1)$$

where the two angles refer to the first and second members of a cascade. The experimental DCO ratios are shown in Table IV and are compared with the calculated values there.

The gamma rays which exhibited Doppler broadening in the 0° singles data were analyzed by the Doppler shift attenuation method (DSAM). The experimental line shapes were compared with the theoretical ones in order to obtain the lifetimes of the states they depopulate. A short run at 155° from the beam direction was taken to search for the presence of small contaminate gamma rays which might be superimposed on the Doppler tails to be analyzed. The theoretical line shapes were calculated with the code DOPCO.[13] In this analysis one starts with the highest level observed and works down in the level scheme. The program includes corrections for known lifetimes of multiple cascades and for slow and fast feeders. To illustrate our DSAM multiple analyses, the fit obtained for the 1124.8 keV 10^+ to 8^+ transition is shown in Fig. 3. One of the critical problems in the line shape analysis is the accuracy of the stopping powers. Since the nuclear stopping powers are not well known at low recoil energies, we scaled the Northcliffe and Schilling values[14] according to the experimental values for alpha particles in the same recoil material. We used the correction

$$(dE/dx)^{HI}_{\text{scaled}} = (dE/dx)^{HI}_{NS} (dE/dx)^{\alpha}_{\text{exp}} / (dE/dx)^{\alpha}_{NS}, \qquad (2)$$

where the experimental stopping powers for alpha particles were taken from Ward *et al.*[15] Since a thin ^{58}Ni target was used in the singles experiment, the recoil nuclei were slowed down in the target and only completely stopped in the Pt backing. The average kinetic energy of the recoil nuclei after leaving the target material was cal-

TABLE II. Attenuation coefficients extracted from the γ-ray angular distributions following the reaction ^{58}Ni(^{12}C,2p)^{68}Ge at 39 MeV.

Level (keV)	E (keV)	J_i	J_f	α_2 (exp)	α_4 (exp)	$(\sigma/J)_2$ (exp)	$(\sigma/J)_4$ (exp)	α_4[a] (calc)
1016	1016	2^+	0^+	0.29(2)	0.033(9)	0.75(4)	0.67(4)	0.022(5)
1778	1778	2^+	0^+	0.21(1)	0.008(7)	0.89(3)	0.93(7)	0.010(3)
2268	1252	4^+	2^+	0.62(4)	0.19(8)	0.41(3)	0.44(7)	0.22(3)
3582	933	5^-	3^-	0.64(12)	0.18(21)	0.36(7)	0.43(20)	0.30(14)
3649	1000	5^-	3^-	0.71(8)	0.28(14)	0.33(6)	0.37(10)	0.38(7)
3696	1428	6^+	4^+	0.67(5)	0.24(9)	0.36(3)	0.39(5)	0.30(6)
4054	405	7^-	5^-	0.77(5)	0.55(18)	0.43(8)	0.30(5)	0.25(7)
	472	7^-	5^-	0.77(5)	0.46(14)	0.43(8)	0.28(5)	0.25(7)
4838	1141	8^+	6^+	0.76(6)	0.59(23)	0.30(5)	0.23(9)	0.41(10)
4958	1075	(8^-)	6^-	0.73(8)	0.35(15)	0.32(5)	0.33(7)	0.37(7)
5050	1354	8^+	6^+	0.83(7)	0.61(21)	0.25(5)	0.23(8)	0.56(14)
5331	1276	(9^-)	7^-	0.79(10)	0.54(27)	0.30(8)	0.25(14)	0.41(20)
5367	1670	8^+	6^+	0.76(12)	0.56(25)	0.34(7)	0.25(9)	0.34(20)
5678	1224	(9^-)	7^-	0.72(12)	0.59(38)	0.34(8)	0.23(17)	0.35(20)
5962	1125	10^+	8^+	0.79(12)	0.57(28)	0.29(10)	0.25(13)	0.41(22)
6215	1165	(10^+)	8^+	0.77(24)	0.97(68)	0.29(25)	0.10(25)	0.41(30)
7045	1715	(11^-)	(9^-)	0.84(17)	0.77(36)	0.24(11)	0.16(14)	0.58(28)
7146	1467	(11^-)	(9^-)	0.61(15)	0.3(3)	0.34(6)	0.3(3)	0.33(8)
7243	1876	(10^+)	8^+	0.62(24)	0.28(34)	0.4(2)	0.4(4)	0.23(20)
7372	1410	(12^+)	10^+	0.63(15)	0.54(43)	0.37(17)	0.25(25)	0.27(12)
7560	1344	(12^+)	(10^+)	0.60(12)	0.40(28)	0.40(11)	0.30(10)	0.24(10)
9172	1800	(14^+)	(12^+)	0.78(25)	0.52(45)	0.28(20)	0.25(20)	0.46(30)

[a] These values of α_4 are calculated from the experimental α_2 values assuming a Gaussian distribution for the population of magnetic substates, i.e., using the σ/J values from the column headed $(\sigma/J)_2$.

culated to be about 1.8 MeV. Since the code DOPCO only accepts one set of stopping powers, several trials were made for values of the stopping powers of the recoil nuclei which changed continuously from the values in ^{58}Ni to those in Pt at about the above energy. Figure 4 shows the correction described above for the Northcliffe and Schilling[14] stopping powers, and the transition line (t) which gave the best fit in the line shape analysis. These results of the mean life measurements are given in Table V. The results of other measurements[6,9] are given for comparison.

The $B(E2)$ values of the low spin states in the ground band of ^{68}Ge are found to be highly collective up to the 6^+ state, as can be seen in Table V. The large experimental errors make it difficult to determine the actual trend but these values are more or less consistent with the IBA (interacting boson approximation models) or the description of these states in terms of a harmonic vibrator. The $B(E2)$ of the $8_3^+ \rightarrow 6^+$ transition, however, has only an enhancement of 3.2 over the single particle value.

The magnitude of the drop-off in collectivity of

TABLE III. Angular distributions in ^{68}Ge from the ^{63}Cu(^{7}Li,2n)^{68}Ge reaction at 18 MeV.

E_γ	A_2	A_4	$J_i^\pi J_f^\pi$	δ	Multipolarity
234	−0.182(16)	−0.03(2)	6^-5^-	0.01(2)	$M1$, $E2$
405	0.275(35)	−0.107(40)	7^-5^-		$E2$
651	−0.177(17)	−0.023(22)	3^+2^+	−0.02(2)	$M1$, $E2$
762	0.094(12)	−0.016(13)	2^+2^+	−0.09(2)	$M1$, $E2$
1016	0.217(10)	−0.038(10)	2^+0^+		$E2$
1252	0.254(10)	−0.034(10)	4^+2^+		$E2$
1314	−0.126(18)	0.025(19)	5^-4^+	0.06(2)	$E1$, $M2$
1381	−0.216(29)	0.017(32)	5^-4^+	−0.01(2)	$E1$, $M2$
1428	0.321(17)	−0.051(23)	6^+4^+		$E2$
1633	−0.189(21)	0.028(26)	3^-2^+	0.01(2)	$E1$, $M2$
1777	0.179(12)	−0.007(14)	2^+0^+		$E2$

TABLE IV. Experimental and theoretical DCO ratios for γ rays in ^{68}Ge.

E_{γ_1}	E_{γ_2}	Exp. R_{DCO}	Spin sequence	Theor.[a] R_{DCO}
738	1016	0.75(25)	0 → 2 → 0	1.00
1252	1016	1.02(4)	4 → 2 → 0	1.00
1633	1016	1.73(14)	3 → 2 → 0	1.85
1055	1777	1.12(18)	4 → 2 → 0	1.00
1428	1252	0.97(5)	6 → 4 → 2	1.00
233	1000	1.51(19)	6 → 5 → 3	1.78
400	404	0.78(16)	7 → 7 → 5	0.88
400	472	0.83(15)	7 → 7 → 5	0.88
400	171	0.51(16)	7 → 7 → 6	0.45
1141	1428	0.96(10)	8 → 6 → 4	1.00
1141	1252	1.02(14)	10 → (8 → 6) → 4	1.00
1075	233	0.52(17)	8 → 6 → 5	0.40
1354	1428	0.96(10)	8 → 6 → 4	1.00
1354	1252	1.08(14)	8 → (6 → 4) → 2	1.00
1670	1428	0.89(13)	8 → 6 → 4	1.00
1125	1141	0.97(9)	10 → 8 → 6	1.00
1125	1428	0.95(14)	10 → (8 → 6) → 4	1.00
1125	1252	0.92(10)	10 → (8 → 6 → 4) → 2	1.00
1165	1354	1.06(13)	10 → 8 → 6	1.00
1409	1125	1.09(23)	12 → 10 → 8	1.00
1344	1165	0.88(18)	12 → 10 → 8	1.00

[a]Calculated using α_2 and δ values from the angular distribution measurements of Table I.

the $8_3^+ \rightarrow 6^+$ transition is not completely understood, but the decrease in the collectivity of this transition can be qualitatively reproduced in an IBA calculation. The large collectivity of the lower two 8^+ states may be explained in the framework of two-quasiparticle-plus-rotor calculations.

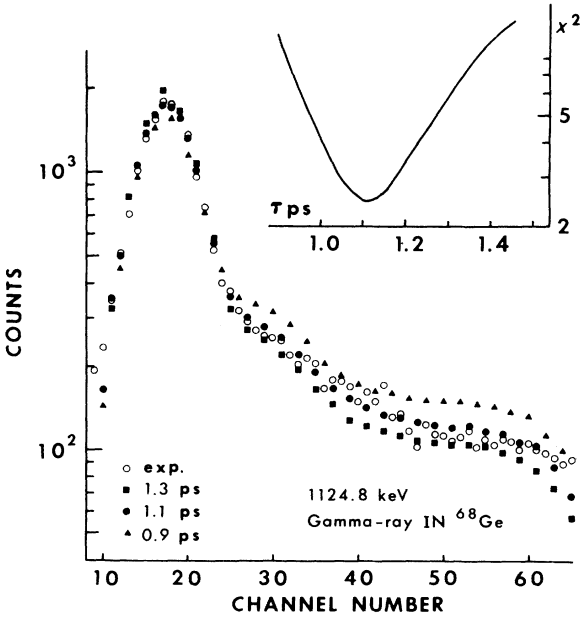

FIG. 3. DOPCO fit of the 1124.8 keV gamma ray.

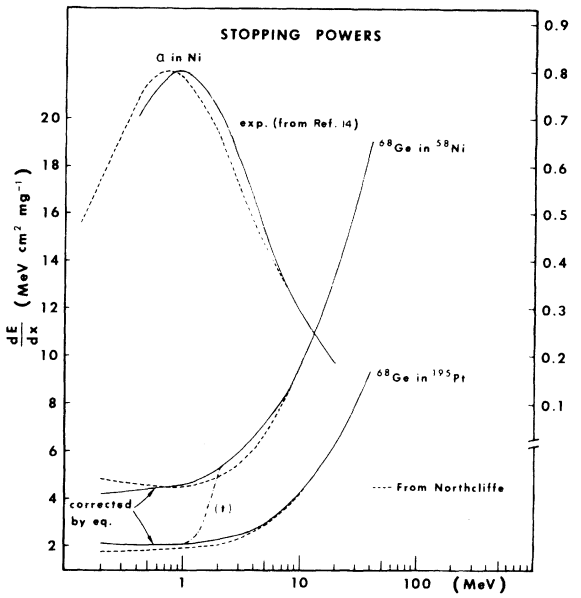

FIG. 4. Stopping powers used in the DSAM analysis. The line (*t*) represents the transition region of the stopping powers adopted in our line shape analysis.

Gamma-ray yields were extracted from singles runs taken at energies from 31.5 to 41.5 MeV in order to select the beam energy to be used in the ^{12}C run. The analysis of excitation functions was later extended to include most of the gamma rays placed in the decay scheme. The yield curves presented in Fig. 5 were used to help establish the spin assignments.

In order to determine the parity of the levels involved, we performed a linear polarization experiment in the reaction ^{63}Cu(^{7}Li, $2n$)^{68}Ge. A Compton polarimeter from Johns Hopkins University, consisting of two Ge(Li) detectors mounted in the same cryostat, was used. An event pulse was obtained from a coincidence between both detectors. The signals from the amplifiers were added and the sum pulse was digitized by the analog-to-digital converter (ADC). The total energy pulse was therefore determined by the gamma rays scattered by either crystal into the other.

The data were accumulated at two angles: the so-called zero degree angle—when the plane defined by the axis of the detectors was coincident with the vertical plane containing the beam direction (reaction plane), and the so-called 90° angle—when the polarimeter was rotated by 90° about its central axis.

The alignment was checked with radioactive sources placed at the position of the beam spot. Since radioactivity gamma rays are unpolarized the counting rate should be the same for both

TABLE V. Mean lives of levels in ^{68}Ge. Previous results are also given for comparison. The $B(E2)_{sp.w.}$ estimates are calculated using the formula $0.59\times10^{-53}A^{4/3}$ (e^2cm^4). Lifetimes are given in picoseconds.

Ex (keV)	J^π	E_γ (keV)	(1975) (Plunger) from Ref. 6	(1976) (Plunger) from Ref. 6	DSAM from Ref. 9	Present work DSAM	Present work $\frac{B(E2)_{exp}}{B(E2)_{sp.w.}}$
1016	2^+	1016	$5.8^{+1.1}_{-0.8}$	2 ± 1	5^{+3}_{-2}	3 ± 1	15 ± 5
2268	4^+	1252	1.3 ± 0.7	<1	$1.2^{+0.4}_{-0.3}$	1.5 ± 0.4	11 ± 3
3696	6^+	1428	≤1	<0.5	$0.7^{+0.2}_{-0.1}$	0.7 ± 0.2	12 ± 3
4838	8^+	1141	$1.9^{+0.8}_{-0.4}$	1.6 ± 0.7	$0.7^{+0.2}_{-0.1}$	1.5 ± 0.3	17 ± 3
5962	10^+	1125			$1^{+0.4}_{-0.2}$	$1.1^{+0.3}_{-0.2}$	25^{+7}_{-5}
5050	8^+	1354				$0.7^{+0.3}_{-0.2}$	16^{+5}_{-6}
5367	8^+	1670			$0.8^{+0.3}_{-0.2}$	$1.2^{+0.4}_{-0.3}$	$3.2^{+1}_{-0.8}$
5351	(9^-)	1276				$1.0^{+0.3}_{-0.2}$	15^{+3}_{-4}

angles. This was also used for energy calibration of the polarimeter. The polarization experiment was run only sufficiently long to establish the parities of the two lowest levels of spin 5 and thus of the bands built on them. The parities of both $I=5$ states were determined to be negative since there is a change in sign between the experimental polarization and the value obtained from the angular distribution of the same gamma ray (see Table VI).

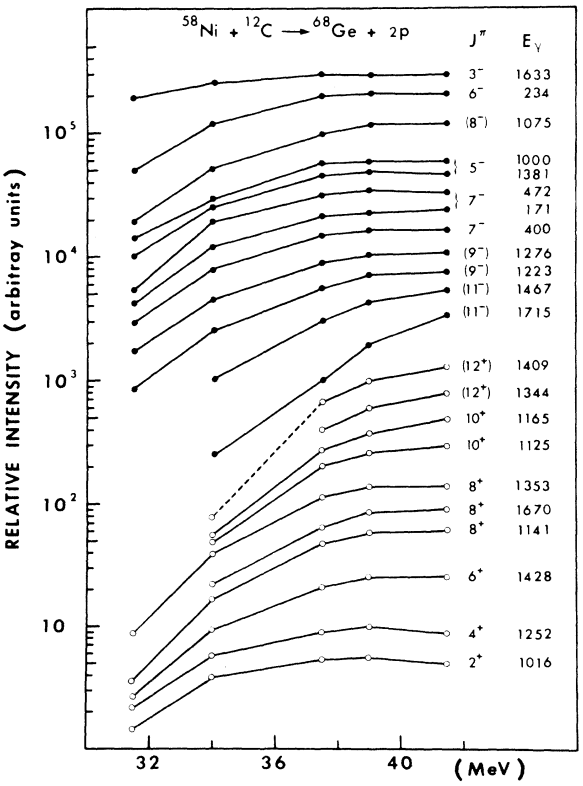

FIG. 5. Yield curves of ^{68}Ge γ rays.

III. ANALYSIS AND RESULTS

The level scheme of the ^{68}Ge deduced in this work is shown in Fig. 2. We have placed a total of 59 transitions into 40 levels of which 19 have not been reported previously. The levels at 1016 keV, 2^+; 1778 keV, 2^+; 2268 keV, 4^+; 2429 keV, 3^+; and 2649 keV, 3^- have been well established previously in a variety of studies including radioactivity[5,10] and transfer reaction work.[5-9,11] Some of the transitions placed in the ^{68}Ge level scheme are doublets and the information obtained from the angular distributions is not completely reliable for these. These γ rays are those with energies of 750.1, 1054.7, 1075.0, and 1096.2 keV; they include contributions from the ^{58}Ni(^{12}C, αp)^{65}Ga reaction. The γ rays at 871.5, 872.4, and 1162.5 keV are doublets with transitions placed in ^{67}Ga; the 233.9 keV transition includes a small component from ^{68}As; and the 358.0 keV γ ray was shown from the coincidence spectra to have contributions from the ^{68}As, ^{67}Ga, and from the Coulomb excitation of ^{196}Pt from the platinum backing. The new levels and established levels, where new information was obtained or inconsistencies clarified, are discussed below. Table VII is a summary of the evidence for the spin and parity assignments. The coincidence results and the evidence for the level assignments are discussed below.

Level at 1754.2 keV: This level had been reported[10,11] as the first excited 0^+ state. The presence of the 738.2 keV γ ray in coincidence with the gate on the 1016 keV γ ray and vice versa confirm the existence of this level. Our experimental

TABLE VI. Results of the polarization experiment. The columns Δ and θ are the experimental asymmetry of the gamma ray and the efficiency of the polarimeter. The values of the polarization are the experimental ones, $P_{exp}=\Delta/\theta$, and the ones obtained from the angular distribution coefficients, P_{AD}.

E_γ	$J_i \rightarrow J_f$	Δ	θ	$P_{exp}=\Delta/\theta$	P_{AD}	Multipolarity
1016	$2 \rightarrow 0$	0.080(9)	0.263(31)	0.304(50)	0.34(2)	$E2$
1252	$4 \rightarrow 2$	0.095(12)	0.225(30)	0.422(78)	0.42(2)	$E2$
1428	$6 \rightarrow 4$	0.125(40)	0.203(30)	0.62(20)	0.55(4)	$E2$
1777	$2 \rightarrow 0$	0.082(51)	0.171(30)	0.48(30)	0.29(2)	$E2$
1314	$5 \rightarrow 4$	0.070(41)	0.217(30)	0.32(19)	−0.33(3)	$E1$
1381	$5 \rightarrow 4$	0.068(25)	0.209(30)	0.32(13)	−0.24(3)	$E1$

value for the DCO ratio (Table IV) is consistent with a $J=0$ spin assignment to this level. It is independently confirmed.[9]

Level at 2832.4 keV: There are some differences in the energy values of this level which is assigned as a 4^+ state.[7,8,10,11] In (p,t) reactions, strongly populated levels at energies of 2.86 MeV (Ref. 8) and 2834 keV (Ref. 11) are reported. More recently, a level was reported in radioactivity work[10] at 2830.8 keV that depopulates by 1052.7 and 1814.7 keV γ rays. These energies are systematically lower than those obtained in the present work by about 2 keV. Nevertheless, we feel that these results are all for the same level which we find at 2832.4 keV. Our analysis of coincidence spectra shows that it is depopulated by a 1054.7-keV γ ray to the 1754.2-keV level and more weakly to the 1016.0-keV level through a 1816.4-keV γ ray. The angular distribution of the 1816.4-keV transition together with the DCO ratio of the 1054.7–1777.7 keV transitions confirm the $J^\pi=4^+$ spin-parity assignment for this state.

Level at 3062.0 keV: A tentative (3^-) level has been proposed at 3065 keV by (p,t) work.[11] Our data definitely establish coincidence between the 587.2 and the 793.9 keV transitions between the 5^- state at 3649.4 keV and the 4^+ yrast state. However, no other transitions were seen to or from an intermediate state. The fact that both γ rays are of the same relative intensity within experimental errors does not allow us to positively assign which transition precedes the other. We place the 793.9 keV transition out of a 3062.0 keV level since (p,t) work reports a similar level with a tentative (3^-) assignment.[11]

Level at 3182.8 keV: The 1405.1 keV γ ray definitely populates the 2^+ state at 1777.6 keV, and its angular distribution coefficients establish the $E2$ nature of the transition, which indicate $J^\pi=4^+$ for this level. Our data are supported by a similar 4^+ assignment from (p,t) work for a 3186-keV level,[11] which we believe is the same level.

Level at 3883.3 keV: This level was only seen to be depopulated by a 233.9 keV transition to the 5^- state at 3649.4 keV. Unfortunately, from our coincidence data, this transition was observed to be a doublet with a transition in ^{68}As. The angular distribution coefficients of this gamma ray were obtained only with the ^{7}Li beam since ^{68}As was not formed in that reaction. The strongest argument in favor of the spin 6 assignment for this state is based on the DCO-ratios measurements. Odd parity is strongly favored by the fact that decays into and out of this level go only to states with known negative parity. If the parity was positive, a much more energetically favored transition to the 4^+ state would be seen.

Level at 4054.2 keV: This state was tentatively reported to be (7^-) by Nolte *et al.*[5] The transitions with energies of 404.8 and 471.8 keV populate the 5^- states at 3649.4 and 3582.4 keV, respectively. Both of these gamma rays have the angular distribution coefficients of quadrupole radiations that indicate 7^- to 5^- transitions. The agreement of the orientation parameter of this level, calculated from these angular distribution coefficients, is good. The yield curves for the 170.7 and 471.8 keV transitions in the ^{63}Cu(^{7}Li, $2n$) reaction studies are also in good agreement with a 7^- spin-parity assignment. Combining all this evidence, we consider the 7^- assignment to be established.

Level at 4454.4 keV: This level has been assigned tentatively as a (7^-) state by Nolte *et al.*[5] and more recently by Morand *et al.*[9] as a 9^- state, but based only on angular distribution results. The presence of the 571.0-keV transition in the various coincidence gates and the presence of the corresponding gamma rays in the 571.0-keV gate establishes that this transition populates the 6^- state at 3883.3 keV. Similarly, other gates establish a 872.4 keV transition from this level to the 3582.4 keV 5^- level. The angular distribution coefficients of the 400.1-keV γ ray to the 7^-, 4054.2-keV level show that it has a large quadrupole contribution, but the placements of the 571.0 and 872.4 keV transitions are consistent with a 7^-,

TABLE VII. Summary of the evidence for the spin and parity assignment.

Level	E_γ	$\gamma(\theta)$ DCO	Yield curves	Decay mode	Polarization	Expected from systematics	Previous assignments	Adopted J^π
1016.0	1016.0	2	2,4	1,2	2^+	2^+	2^+[2,4,5,7,10]	2^+
1754.2	738.2	0		≤4		$0^+,2^+$	0^+[2,10]	0^+
							0^+[7]	
1777.6	761.6	2		1–2	2^+	0–2–4	2^+[4,5,7]	2^+
	1777.7							
2268.1	1252.2	4	2,4	≤4	4^+	4^+	4^+[2,4,5,7,10]	4^+
2428.8	651.1	3		≤4			3^+[2,4,7]	3^+
	1412.9						3[5]	
2456.3	702.1			1,2			2^+[7]	2^+
2649.1	871.5	3	<4	≤4			3^-[2,4,5,7,10]	3^-
	1633.1							
2947.5	1169.8			≤4			2,3,4[7]	(2^+)
3040.8	611.8	(4)					2,3,4^+[7]	
	1263.4			1,2,3,4^+				
3062.0	793.9			3,4,5,6			(3^-)[10]	
3086.0	1331.8			1,2			(2^+)[7]	$1^+,2^+$
3182.8	1405.1	2,4		≤4			4^+[10]	4^+
3399.7	1622.2			1,2^+				$1^+,2^+$
	1645.3							
3582.4	750.1	5		2,3,4,5	5^-	5^-	5^-[4,5]	5^-
	933.2						(5^-)[2]	
	1314.3							
3649.4	587.2	5	5–7	2,3,4,5	5^-	5^-	5^-[4,5]	5^-
	1000.5						(5^-)[2]	
	1381.3							
3675.6	1246.8							(5^+)
3696.4	1428.2	6	6	6–8	6^+	8^+	6^+[2,4,5]	6^+
3883.3	233.9	6	5–7	4–7			6^-[2,4,5]	6^-
4054.2	170.7	7	6–8	4,5,6,7^-		7^-	7^-[4,5]	7^-
	358.0						(7^-)[2]	
	404.8							
	471.8							
4454.4	400.1	7	6–8	5,6,7		7^-	7^-[4]	7^-
	571.0						9^-[5]	
	872.4							
4659.9	605.7	7,9	5–9					
4837.6	783.2	(8)	8	4–8		8^+	8^+[4,5]	8^+
	1141.3							
4958.2	903.8	(8)	6–9	5–8		8^-		(8^-)
	1075.0							
4999.4	1303.0			4–8				(6^+)
5050.0	1353.8	(8)	7–9	4–8				8^+
5150.4	1096.2							
5330.6	1276.4	7,9	7–10	5–9		9^-		(9^-)
5366.8	1670.4	(8)	7–9	4–8		8^+		8^+
5678.2	1223.7	(9)	8–10	5–9		(9^-)		9^-
5822.4	491.8							
	1162.5							
5874.0	1036.5			6–10				
5962.3	631.6	(10)	10–12	6–10		10^+		10^+
	1124.8							
6215.2	1165.4	(10)	10–12	6–10		10^+		(10^+)
7045.3	1714.7	(11)	>9	7–11		11^-		(11^-)
7145.6	1467.4	(11)	>9	7–11		11^-		(11^-)
7242.8	1876.0	(10)		6–10		10^+		(10^+)
7371.9	1409.6	(12)	≥10	8–12		12^+		(12^+)
7559.6	1344.4	(12)	≥10	8–12		12^+		(12^+)
9172.2	1800.4	(14)		10–14		14^+		(14^+)

but not a 9^-, assignment. The experimental DCO ratios that involve the 400.1-keV transition and its yield curve are the other basis for our spin-parity assignment of 7^-.

Level at 4659.9 keV: The new level at 4659.9 keV is observed to decay to the 7^- state at 4054.9 keV through a 605.7-keV γ ray. The angular distribution of the 605.7-keV γ ray is more consistent with $\Delta J = +2$. This leads us to suggest that this level has $J^\pi = (9^-)$.

Levels at 4837.6, 5050.0, and 5366.8 keV: These three levels which feed the 6^+ yrast state are established as $J^\pi = 8^+$. Of these, only the 4837.6-keV level was previously reported[5,6] with a tentative 8^+ assignment.[6] The angular distribution of these gamma rays are very similar to and characteristic of 8^+ to 6^+ pure quadrupole transitions. The DCO ratios that involve these transitions (see Table IV) support the 8^+ assignment. The relative yield curves for these gamma rays also support 8^+ assignments for these levels. One problem that always arises when analyzing angular distribution data is that a $6^+ \rightarrow 6^+$ transition with $\delta(E2/M1) = 1$ is also compatible with the angular distribution results and compatible with the experimental DCO ratios (taken at a $0° - 90°$ geometry) within the experimental errors. However, it would be highly unusual to find above the

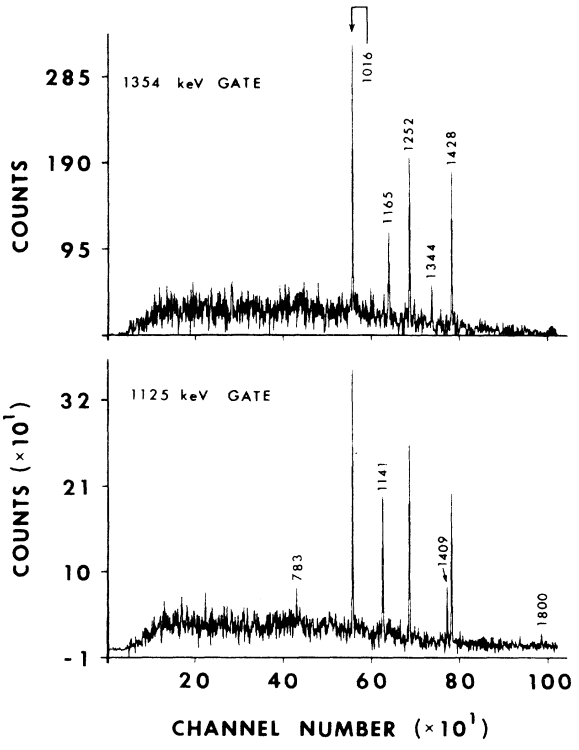

FIG. 6. Spectra in coincidence with 1125-and 1354-keV keV γ rays.

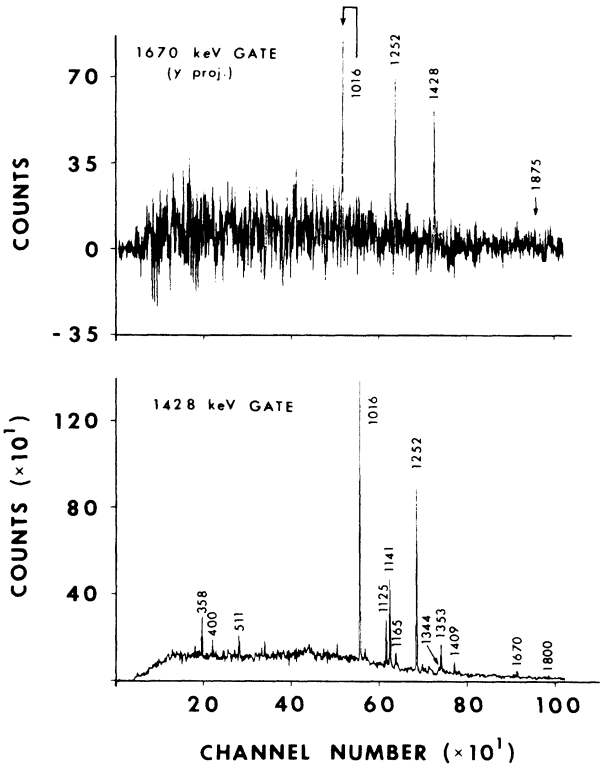

FIG. 7. Spectra in coincidence with 1670-and 1428-keV γ rays.

yrast 6^+ level three 6^+ states, each decaying by transitions with the same δ and none decaying to any lower 4^+ state. More importantly, the yield curves definitely favor an 8^+ over a 6^+ assignment. Thus, we consider the 8^+ assignments to be definite, based on the above evidence for each of these states. Coincidence gates set on the 1353.6 and 1124.8 keV γ rays are shown in Fig. 6 These gates illustrate the placement of the γ rays in these side bands. The continuation of the ground-state band is illustrated in Fig. 7, which shows the gates on the 1670 keV transition. The gate on the 1428-keV γ ray ($6^+ \rightarrow 4^+$) also shown in Fig. 7 clearly shows the 1141-, 1353-, and the 1670-keV γ rays, which are assigned to the decays of these three 8^+ states.

Level at 4958.2 keV: This new level decays to the 6^- level by 1075.0-keV gamma ray. Then angular distribution coefficients of this transition and the DCO ratio between the 1075.0 and 233.9 keV transitions are consistent with a $J = 8$ spin assignment for this level. Since it decays to only odd-parity levels, odd parity is tentatively assigned.

Level at 4999.4 keV: Coincidence data show that this new level feeds the 6^+ state at 3696 keV through a 1303.0-keV gamma ray. This transition is too weak for accurate spin assignment. A tentative (6^+) assignment is based on its simple decay

and on the fact that one may expect partially aligned 6^+ levels at this energy.

Level at 5150.4 keV: This level is established only by the 1096.2-keV transition which is a doublet with a 1096.0-keV γ ray in ^{69}Ga. Since most of its intensity comes from this other channel, it is not possible to make even a tentative spin assignment.

Levels at 5330.6 and 7045.3 keV: These levels are tentatively assigned as 9^- and 11^- respectively. The gate in the 1276.4-keV γ ray (see Fig. 8) shows that it feeds the 7^- level at 4054.2 keV and defines the 5330.6-keV level. The coincidence gate on the 1714.7-keV γ ray also supports the establishment of these levels. The angular distributions of the 1276.4- and the 1714.7-keV γ rays (see Table I) clearly show that these transitions are $\Delta J = 2$. This leads us to consider these levels as members of an odd-spin negative parity band.

Levels at 5678.2 and 7145.6 keV: The gates on the 1467.7- and 1223.7-keV γ rays establish these as new levels above the 4454.4 keV 7^- level with no branching to other levels. The angular distributions and yield curve data are the basis for our spin-parity assignments of (9^-) and (11^-), respectively.

Level at 5822.4 keV: This level is established by the coincidence relations with the 491.8 and the 1162.5 keV transitions. The presence of these two γ rays in the corresponding gates and the good agreement of the energy sums definitely defines this level.

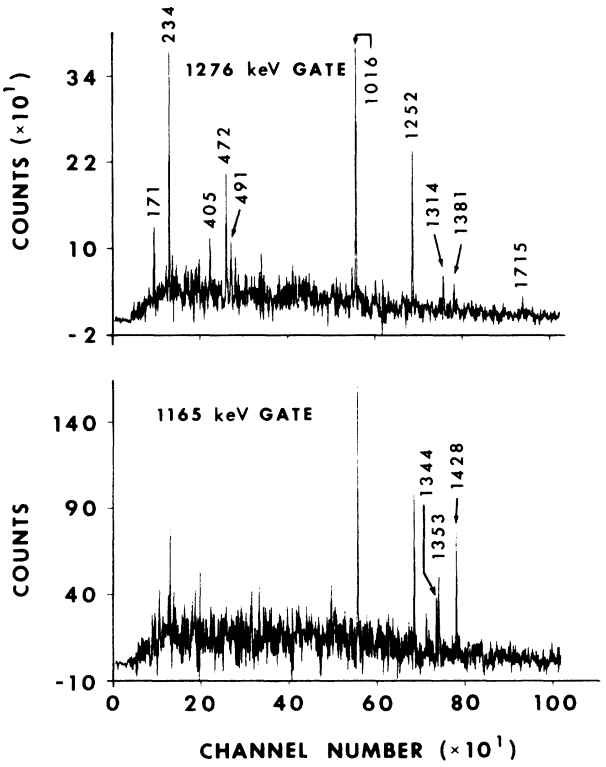

FIG. 8. Spectra in coincidence with 1276-and 1165-keV γ rays.

Level at 5874.0 keV: The 1036.5 keV γ ray from this new level to the 8^+ level at 4837.6 keV is in strong coincidence with the 1141.3 keV γ ray and the subsequent transitions. The presence of the 1036.5 keV γ ray in the 1141.3 keV gate definitely places it as a feeder of the 4837.6 keV level.

Levels at 5962.3, 7371.9, and 9172.2 keV: The gate on the 1124.8-keV gamma ray is shown in Fig. 6 to illustrate the information that established the new levels which form a band built on the 4837.6-keV, 8^+ level. The angular distribution of the 1124.8-keV transition and the DCO ratio for this transition, coupled with the yield curve, establish the 5962.3 keV as 10^+. Based on the systematics of yrast cascades, the 7371.9-keV level is tentatively assigned (12^+). This assignment is consistent with the angular distribution and yield curve data, but the errors are larger than for the 1124.8-keV level, so this (12^+) assignment is considered tentative. In the 1024.8-keV gate, the 1800.4-keV transition is clearly seen. The 1409.6-keV gate is weak and the presence of the 1800.4-keV gamma ray is allowed, but not established, by this gate. From the systematics of yrast cascades, we favor the placement of the 1800.4-keV transition as depopulating a tentative (14^+) level at 9172.2 keV to the (12^+) level at 7371.9 keV, rather than as a transition to the 10^+, 5962.3 keV level.

Levels at 6215.2 and 7559.6 keV: Gates on the 1354.4, 1165.4, and 1344.4 keV transitions (see, for example, Figs. 6 and 8) establish these new levels as members of a band built on the 8^+ level at 5050.0 keV. The angular distribution, DCO ratio, and yield curve data strongly support 10^+ and 12^+ spin-parity assignments, however, being cautious, the 12^+ transition is listed as tentative.

Level at 7242.8 keV: The gate on the 1876.0-keV transition indicates that a transition from this level at least feeds the 6^+, 3696.4 keV level and probably feeds the 8^+, 5366.8 keV level. In the weak 1670.4-keV gate, the 1876.0-keV transition is so weak that we cannot say whether or not it is definitely present. Systematics favor this transition as feeding the 5366.8-keV level from a 10^+ one, and thus a tentative (10^+) level is assigned at 7242.8 keV.

IV. LEVEL STRUCTURE OF ^{68}Ge

The low-energy ($\lesssim 2.5$ MeV) level scheme of ^{68}Ge was previously interpreted as typical for a vibrational-like nucleus[2,5,10] with the two phonon 0^+, 2^+, 4^+ triplet at 1754.2, 1777.6, and 2268.1

keV, respectively. In fact, the centroid of these three states, 2071 keV, lies at approximately twice the energy of the 2^+ first excited state; there are no observed transitions between the so-called 2-phonon states, and the $B(E2)$ decay from the 2_2^+ to the 2_1^+ level is about 100 times stronger than that for the 2_2^+ to 0^+ ground-state transition, based on the Weisskopf estimates for single particle $E2$-transition rates.

Very little theoretical work has been published about ^{68}Ge. Guilbault *et al.*[11] have presented calculations in which ^{68}Ge is described as a vibrating core (^{40}Ca or ^{56}Ni) with a number of phonons $N<4$ coupled to two-quasiparticle states by a dipole-plus-quadrupole interaction.

Shell-model calculations for ^{68}Ge were also made,[11] considering ^{56}Ni and ^{64}Ge as an inert core with the $g_{9/2}$ orbital available only for neutrons. These investigations appear unsuccessful in reproducing the experimental data.

The different structures of the $^{68-76}$Ge isotopes were analyzed by Ardouin *et al.*[16] in terms of an oblate-to-prolate transition. They performed constrained Hartree-Fock calculations using Skyrme's effective interaction. The potential-energy curves that they obtained show a transition from an oblate shape in ^{68}Ge to a prolate shape in ^{72}Ge.

From our results the feeding of the 6^+ yrast state is extremely unusual with population from three 8^+ levels. Above this state the structure of the ^{68}Ge levels separates into definite bands. The situation for high spin states seems similar to what has been observed in the Ba and Pd isotopes.[17,18] They have been interpreted in terms of the alignment of the angular momentum of two high-spin, low Ω particles with the rotation of the core.

Here we report details of our two-quasiparticle-plus-rotor calculations for ^{68}Ge. This type of calculation is described in detail by Flaum and Cline.[19] Their calculations have been modified to include explicitly a variable moment of inertia (VMI). The dependence of the moment of inertia on the total angular momentum, described elsewhere,[20] is based on the VMI model of Mariscotti, Scharff-Goldhaber, and Buck.[21] The two parameters required were obtained from a fit to the zero-quasiparticle band of ^{68}Ge and then varied somewhat to obtain better energy spacing in the two-quasiparticle bands. The one-quasiparticle wave functions for the two-quasiparticle calculations were obtained from an oscillator Nilsson model calculation, assuming a deformation of $\delta = 0.1$. The shell model parameters κ and μ were adjusted so that the $g_{9/2}$, $f_{5/2}$, $p_{1/2}$, and $p_{3/2}$ level positions at zero deformation corresponded to those determined by Reehal and Sorenson.[22]

TABLE VIII. Shell model parameters used in the two-quasiparticle RAL model calculation.

	N	κ	$\delta=0.1$ μ	λ (Fermi energy)
ν	4	0.0600	0.500	45.5
	3	0.0400	0.55	45.2
π	4	0.0700	0.38	45.5
	3	0.0700	0.31	44.7

The values of κ and μ used for the four different Nilsson calculations are given in Table VIII. Two-quasiparticle basis wave functions were then constructed by coupling quasiparticle spins and antisymmetrizing. Finally, the Coriolis matrix elements between different basis states were calculated, and final energies and wave functions were obtained by performing a matrix diagonalization. Actually four independent calculations are required for the interpretation of the ^{68}Ge level scheme; namely, for positive and negative parity two-quasineutron and two-quasiproton states. The calculations do not contain a residual interaction which can mix two-quasineutron and two-quasiproton states. Thus the results of the combined calculations must be regarded as approximate for those cases where two states of the same spin and parity, but from different subsets, are predicted to be close in excitation energy.

The results of the calculated energies are compared to experimental energies in Fig. 9. The absolute energies of the two 8^+ and two 5^- states from the four calculated subsets have been shifted (170 keV in the worst case) to coincide with the data. All other relative energies are unchanged. The calculation describes the yrast features of the level scheme very well. The most significant aspect of the results is that, independent of any fine parameter adjustments, the calculations unambiguously identify the nature of the main cascades observed. The positive parity states result from particles in $g_{9/2}$ orbitals. Because of the neutron excess, the neutron Fermi surface is closer to the $g_{9/2}$ Nilsson orbitals than is the proton Fermi surface. Thus the lower-lying 8^+ state is identified as being of two-quasineutron origin, with the second 8^+ state being of two-quasiproton origin. The next 8^+ two-quasiparticle states are predicted to be more than 1 MeV higher. Both bands are well-decoupled, as evidenced by the predicted energies of the odd-spin states.

The identification of the odd-spin negative parity states is just as definite. For both two-quasineutron and two-quasiproton states, one quasi-

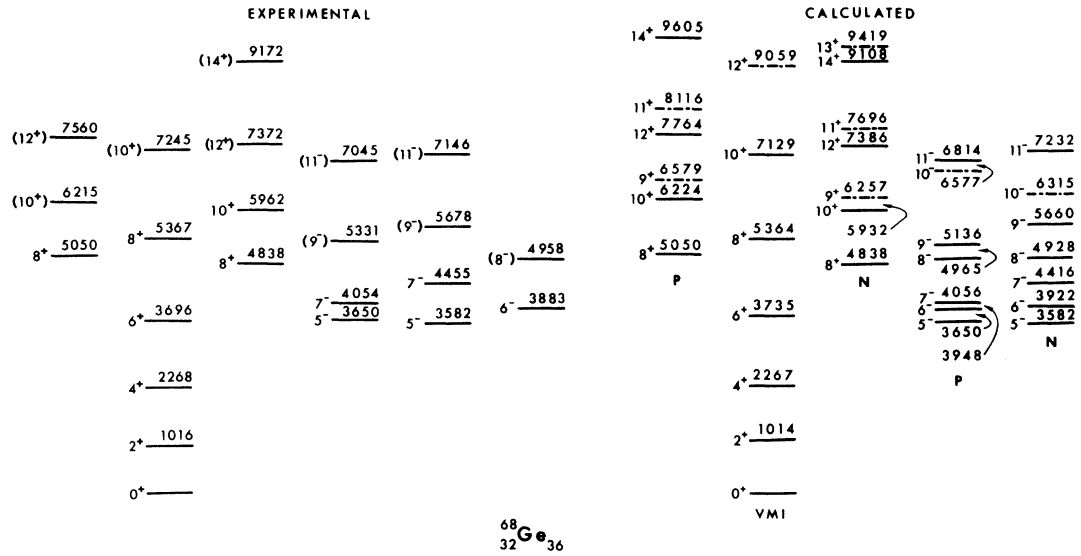

FIG. 9. (a) The levels in $^{68}_{32}$Ge deduced from in-beam spectroscopy following the ^{58}Ni(^{12}C, $2p$) and ^{63}Cn(^{7}Li, $2n$) reactions. (b) Calculated levels based on a two-quasiparticle-plus-rotor model are shown for comparison with the experimental data.

particle occupies a $g_{9/2}$ Nilsson orbital and the other a $p_{1/2}$, $p_{3/2}$, or $f_{5/2}$ Nilsson orbital. There are, however, two effects which result in two-quasineutron states and two-quasiproton states exhibiting different characteristics. The proton Fermi surface is lower than the neutron Fermi surface, and the Nilsson level schemes for the two cases are different for the $N=3$ orbitals. The negative parity orbitals near the neutron Fermi surface are the high Ω states from $f_{5/2}$ and $p_{3/2}$ orbitals, with the singe $p_{1/2}$ orbital close by. Thus the resulting yrast band that develops is not decoupled, and exhibits a regular $\Delta I=1$ level sequence built on a 5^- state of mixed parentage. The proton Fermi surface, on the other hand, lies close to the $\Omega=\frac{1}{2}$ orbital of $f_{5/2}$ parentage and the $\Omega=\frac{3}{2}$ orbital of $p_{3/2}$ parentage, with the $p_{1/2}$ orbital far away. This does result in a low-lying 5^- state, but the 7^- state is much more decoupled and plays the role of the bandhead. The signature of this is the compression in energy of the 5^- and 6^- states below the 7^- state, with a regular band which is partially decoupled above the 7^- state. This definite contrast between the predicted behavior of two-quasineutron and two-quasiproton bands is readily apparent in the experimental level scheme (see Fig. 9).

The observed 6^- and 8^- states could correspond to either two-quasineutron or two-quasiproton, from the calculation, and probably are mixed states. It seems likely that considerable mixing exists between all the low-lying 5^-, 6^-, 7^-, and 8^- states, which may explain their observed branchings.

In conclusion, in contrast to ^{72}Se, ^{74}Se where the even-parity yrast bands exhibit "forward bending" of the moment-of-inertia plot with no forking, triple forking is observed at 8^+ in ^{68}Ge, with backbending at the two lowest 8^+ states, to indicate that a variety of nuclear motions are occurring in this region. The bands built on the two lowest 8^+ states and the three new odd parity bands in ^{68}Ge can be explained in the framework of RAL model calculations.

Arima and Iachello[24] have proposed an interacting boson approximation (IBA) model, which provides a unified description of collective nuclear states in terms of a system of interacting bosons. These bosons are identified with Fermion pairs coupled to $L=0$ (s) and to $L=2$ (d). The negative-parity states are formed by the inclusion of one 3^- (f) boson.

We have made calculations of level energies of positive- and negative-parity bands of ^{68}Ge, using the computer code PHINT.[24] For ^{68}Ge, there are 6 active bosons, formed by 4 protons (particle) pairs and 8 neutron (particle) pairs outside of closed shells. In the program PHINT, energy levels are found by diagonalizing the Hamiltonian, and the values of the two-body matrix elements coupling the s and d bosons are adjusted in a least-squares fit to the experimental positive-parity level energies. Next, with these matrix elements held constant, the matrix elements coupling the single f boson to the s and d bosons are adjusted in a least-squares fit to the experimental negative-parity level energies.

Values of the parameters in PHINT (Ref. 24)

giving the best fit are the following: HBAR= =1.0608 MeV, $C(0)=0.0879$ MeV, $C(2)=-0.424$ MeV, $C(4)=0.211$ MeV, $F=0.0825$ MeV, $G=-0.038$ MeV, $CH1=0.000$ MeV, $CH2=0.000$ MeV, HBAR3 = 2.649 MeV, $F3=0.216$ MeV, $D(1)=0.4770$ MeV, $D(2)=0.465$ MeV, $D(3)=0.104$ MeV, $D(4)=-0.4453$ MeV, $D(5)=-0.0837$ MeV, and EPSD = −0.100. The parameters $F3$, $D(1)$, $D(2)$, $D(3)$, $D(4)$, and $D(5)$ are not completely independent. They are calculated using K and K' equal to Q_d+Q_f and L_d and L_f interactions. In the fitting procedure, the level energies fitted are the 0_1^+, 2_1^+, 2_2^+, 2_3^+, 3_1^+, 4_1^+, 4_2^+, 6_1^+, 8_3^+, and 10_3^+ experimental states. These states and the negative-parity states were given weights proportional to $1/E_L$, while the other positive-parity level energies were given weights proportional to $0.1/E_L$.

Level energies calculated by this model are compared with experimental values in Table IX. The calculations reproduce very well the ground-state band and most of the other low-spin positive-parity states. This model, with only s and d bosons, has only one low energy 8^+ level and cannot explain the bands built on the two lowest 8^+ states, which have quite different structure. For the negative-parity states the differences between the calculated and experimental energies are larger than for the low-spin yrast states, with a large oscillating difference for the second band, as one can see from Table IX. In particular, note that the calculations do not reproduce the different $5^- - 7^-$ spacings in the two bands in contrast to the two quasiparticle plus rotor calculations, where these differences are nicely reproduced.

The calculation of the quasigamma band levels with the IBA is better than the calculation for the negative-parity states. However, the choice for the quasigamma band 4^+ level is not unique since three 4^+ states are identified at approximately the right energy.

Zhang and Zhang[23] have also carried out rotation-aligned calculations in an HFB-cranking model. Their calculations similarly show that the two lowest 8^+ levels are primarily RAL $(g_{9/2})^2$ two quasineutron and two quasiproton bands. In a separate publication they[23] suggest that the third 8^+ level at 5367 keV may not be a member of the ground band but a member of a band with different deformation. However, they used the $B(E2)$ of the 8_3^+ level in their argument and, in fact, the drop in this $B(E2)$ may be evidence instead for the predicted IBA drop-off at high spin.

The $B(E2)$ values also can be calculated from the IBA using the FBEM code.[24] However, one needs the $B(E2,\ 2_2^+ \to 0^+)$ and $B(E2,\ 2_1^+ \to 0^+)$ values for normalization purposes. In the case of ^{68}Ge, the $B(E2,\ 2_2^+ \to 0^+)$ and the $B(E2,\ 2_1^+ \to 0^+)$ are not known very accurately. Yet we have tried the calculations with several possible values consistent with the experimental values. For this reason, the results are not unique and one can only conclude from this calculation that there is a drop in $B(E2,\ 8_3^+ \to 6^+)$ compared to the $B(E2)$ values of the lower spin members of the ground band. Indeed, this may be the first definite evidence for the drop-off in collective strength in IBA because of the finite numbers of bosons. An earlier report[25] in ^{78}Kr for such an IBA drop-off in $B(E2)$ at higher spin has now been shown to be incorrect because the 14^+ and 16^+ states, where a big drop is observed, are not members of the ground band.[26]

TABLE IX. Energy levels of ^{68}Ge calculated in an IBA model.

J^π	E_{exp} (keV)	E_{calc} (keV)	Difference (keV)
0^+	0	0	0
2^+	1016	1038	−22
4^+	2268	2269	−1
6^+	3696	3698	−2
8^+	5367	5339	28
(10^+)	7243	7259	−16
3^-	2649	2591	58
5^-	3582	3385	197
7^-	4454	4420	34
(9^-)	5678	5618	60
(11^-)	7146	6696	150
5^-	3649	3617	32
7^-	4054	4172	−118
(9^-)	5331	5224	107
(11^-)	7045	7560	−515
6^-	3883	3829	54
2^+	1778	1727	51
3^+	2429	2477	−48
(4^+)	3041	3217	−176
(5^+)	3676	3592	84
0^+	1754	1764	−10
2^+	2456	2470	−14
4^+	2832	2850	−18
4^+	3183	3314	−131

V. SUMMARY

A surprising large number of collective band structures have been observed near the yrast line in ^{68}Ge. The low-spin ($I^\pi \leq 6^+$) positive-parity states, including the ground and quasigamma bands are well described in terms of the interacting boson approximation. The triple forking in the yrast band above 6^+ is not explained in an IBA model with only s and d bosons, but can be nicely explained as the coupling of two-quasiproton and two-quasineutron excitations to the collective degrees of freedom which describe the low lying

states. The drop-off in the $B(E2)$ of the 8_3^+ level (which is thought to be a ground band level) may be the first definite evidence for the drop-off at high spins predicted by the IBA. This reduction in collectivity at high spin is a result of finite number of boson degrees of freedom. This is the first time both proton and neutron RAL bands built on the same orbital have been observed in one nucleus.

Negative parity states are predicted in collective models (as octupole vibrations or as octupole, f-boson, couplings). However, the energy level spacings, particularly in the two odd-spin, negative-parity bands, are best explained in the two quasiproton plus rotor calculations to suggest that these bands are two-quasiparticle excitations. Indeed, two-quasiproton and two-quasineutron excitations coupled to collective degrees of freedom (IBA for example) reproduce the major features of the high spin states in ^{68}Ge.

ACKNOWLEDGMENTS

The research at Vanderbilt University is supported in part by the U.S. Department of Energy under Contract No. DE-AS05-76ER0534, and at Oak Ridge National Laboratory through Contract No. W-7405-eng-26 with Union Carbide Corporation. The research at Brookhaven National Laboratory is also supported by the U.S. Department of Energy. The research performed at Purdue University was supported in part by a grant from the National Science Foundation.

---

*On fellowship from Instituto Nacional de Investigãco Cientifica, Portugal.
†On leave from Delft Technological University, The Netherlands.
‡Present address: Physics Department, Michigan State University, East Lansing, Michigan.
§On leave from Institute for Nuclear Study, Tokyo.
¶On leave from Coimbra University, Portugal.

[1]A. P. de Lima *et al.*, Phys. Lett. 83B, 43 (1979).
[2]A. P. de Lima *et al.*, *Proceedings of the International Conference on Selected Topics in Nuclear Structure Dubna, U. S. S. R., 1976,* edited by V. G. Soloviev, Vol. I (Dubna, 1976), p. 194.
[3]A. P. de Lima *et al.*, *International Conference on Nuclear Physics, Tokyo, 1977,* edited by T. Marumori (Physical Society of Japan, Tokyo, 1978), p. 276.
[4]J. H. Hamilton, R. L. Robinson, and A. V. Ramayya, *Nuclear Interactions*, edited by B. A. Robson (Springer, Berlin, 1979), p. 253.
[5]E. Nolte, Y. Shida, W. Kutschera, R. Prestele, and H. Morinaga, Z. Phys. 268, 267 (1974); E. Nolte, W. Kutschera, Y. Shida, and H. Morinaga, Phys. Lett. 33B, 294 (1970).
[6]G. M. Gucinsky, M. A. Ivanov, I. Kh. Lemberg, and A. S. Mishiv, *Proceedings of the Nuclear Structure Conference, Leningrad, 1975* (Academy of Sciences, USSR), p. 376; I. Kh. Lemberg, private communication.
[7]T. H. Hsu, R. Fournier, B. Hird, J. Kroon, G. C. Ball, and F. Ingebretsen, Nucl. Phys. A179, 80 (1972).
[8]J. R. Shepard, R. Graetzer, and J. J. Kraushaar, Nucl. Phys. A197, 17 (1972).
[9]C. Morand, J. F. Bruandet, A. Giorni, and T. U. Chan, J. Phys. (Paris) 38, 11 (1977).
[10]R. C. Pardo, C. N. Davids, M. J. Murphy, E. B. Norman, and L. A. Parks Phys. Rev. C 15, 1811 (1977).
[11]F. Guilbault, D. Ardouin, R. Tamisier, P. Avignone, M. Vergnes, G. Rotbard, G. Berrier, and R. Seltz, Phys. Rev. C 15, 894 (1977).
[12]K. S. Krane, R. M. Steffen, and R. M. Wheeler, Nucl. Data Tables 11, 351 (1973).
[13]DOPCO, Oak Ridge National Laboratory Computer Library.
[14]L. C. Northcliffe and R. F. Schilling, Nuclear Data Tables 7, Nos. 3 and 4 (1970).
[15]D. Ward, J. S. Forster, H. R. Andrews, I. V. Mitchell, G. C. Ball, W. G. Davies, and G. J. Costa, Report No. AECL-4914.
[16]D. Ardouin, R. Tamisier, M. Vergnes, G. Rotbard, J. Kalifa, G. Berrier, and G. Grammaticos, Phys. Rev. C 12, 1745 (1975).
[17]C. Flaum, D. Cline, A. W. Sunyar, O. C. Kistner, Y. K. Lee, and J. S. Kim, Nucl. Phys. A264, 291 (1976).
[18]J. A. Grau, L. E. Samuelson, F. A. Rickey, P. C. Simms, and G. J. Smith, Phys. Rev. C 14, 6 (1976).
[19]C. Flaum and D. Cline, Phys. Rev. C 14, 1224 (1976).
[20]L. E. Samuelson, J. A. Grau, F. A. Rickey, and P. C. Simms (unpublished).
[21]M. A. Mariscotti, G. Scharff-Goldhaber, and B. Buck, Phys. Rev. 178, 1864 (1969).
[22]B. Reehal and R. Sorensen, Phys. Rev. C 2, 819 (1970).
[23]Zhang Jing Ye, private communication.
[24]A. Arima, T. Otsuka, F. Iachello, and I. Talmi, Phys. Lett. 66B, 205 (1977); A. Arima and F. Iachello, Ann. Phys. (N.Y.) 99, 253 (1976); 111, 201 (1978).
[25]H. P. Hellmeister, J. Keinonen, K. P. Lieb, R. Rascher, R. Ballini, J. Delaunay, and H. Dunont, Phys. Lett. 85B, 34 (1979).
[26]R. B. Piercey, A. V. Ramayya, J. H. Hamilton, and R. L. Robinson, Summer School in Varna, Bulgaria, 1980 (to be published).